Science of the Total Environment 904 (2023) 166783

Contents lists available at ScienceDirect

Science of the Total Environment

journal homepage: www.elsevier.com/locate/scitotenv

Deposition behaviors of carboxyl-modified polystyrene nanoplastics with goethite in aquatic environment: Effects of solution chemistry and organic macromolecules

Ruiyin Xie [a,b,1], Xiaohui Xing [a,1], Xin Nie [b,*], Xunsong Ma [c], Quan Wan [b,d], Qingsong Chen [a], Zixiong Li [a], Jingxin Wang [a,*]

[a] Guangdong Provincial Engineering Research Center of Public Health Detection and Assessment, School of Public Health, Guangdong Pharmaceutical University, Guangzhou 510310, China
[b] State Key Laboratory of Ore Deposit Geochemistry, Research Center of Ecological Environment and Resource Utilization, Institute of Geochemistry, Chinese Academy of Sciences, Guiyang 550081, China
[c] School of Chemistry and Materials Science, Guizhou Normal University, Guiyang 550001, China
[d] CAS Center for Excellence in Comparative Planetology, Hefei 230026, China

HIGHLIGHTS

- Increasing pH suppress the deposition of COOH-PSNPs.
- Adding cations or anions reduce deposition extent of COOH-PSNPs with goethite.
- Organic macromolecules inhibit the deposition of COOH-PSNPs with goethite.
- Inhibiting capacity for deposition of COOH-PSNPs follow the sequence of SA > HA > BSA.
- Electrostatic interactions play an leading role in the interaction.

GRAPHICAL ABSTRACT

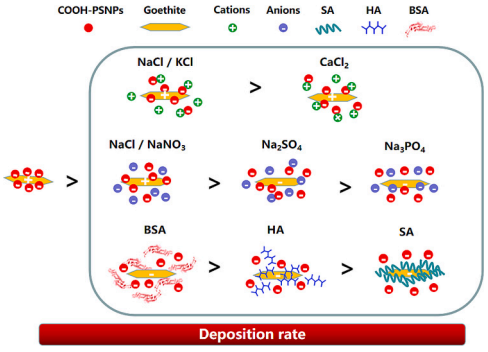

ARTICLE INFO

Editor: Yi Yang

Keywords:
Carboxyl-modified polystyrene nanoplastics
Goethite
Deposition
Cations or anions
Organic macromolecules

ABSTRACT

The ubiquitous nanoplastics (NPs) in the environment are emerging contaminants due to their risks to human health and ecosystems. The interaction between NPs and minerals determines the environmental and ecological risks of NPs. In this study, the deposition behaviors of carboxyl modified polystyrene nanoplastics (COOH-PSNPs) with goethite (α-FeOOH) were systematically investigated under various solution chemistry and organic macromolecules (OMs) conditions (i.e., pH, ionic type, humic acid (HA), sodium alginate (SA), and bovine serum albumin (BSA)). The study found that electrostatic interactions dominated the interaction between COOH-PSNPs and goethite. The deposition rates of COOH-PSNPs decreased with an increase in solution pH, due to the enhanced electrostatic repulsion by higher pH. Introducing cations or anions could compress the electrostatic double layers and compete for interaction sites on COOH-PSNPs and goethite, thereby reducing the deposition

* Corresponding authors.
E-mail addresses: niexin2004@163.com (X. Nie), wjxdaxue@163.com (J. Wang).
[1] Both the authors contributed equally to this work.

https://doi.org/10.1016/j.scitotenv.2023.166783
Received 6 July 2023; Received in revised form 18 August 2023; Accepted 1 September 2023
Available online 2 September 2023

rates of COOH-PSNPs. The stabilization effects, which were positive with ions valence, followed the orders of NaCl ≈ KCl < $CaCl_2$, $NaNO_3$ ≈ NaCl < Na_2SO_4 < Na_3PO_4. Specific adsorption of SO_4^{2-} or $H_2PO_4^-$ caused a potential reversal of goethite from positive to negative, leading to the electrostatic forces between COOH-PSNPs and goethite changed from attraction to repulsion, and thus significantly decreasing deposition of COOH-PSNPs. Organic macromolecules could markedly inhibit the deposition of COOH-PSNPs with goethite because of enhanced electrostatic repulsion, steric hindrance, and competition of surface binding sites. The ability for inhibiting the deposition of COOH-PSNPs followed the sequence of SA > HA > BSA, which was related to their structure (SA: linear, semi-flexible, HA: globular, semi-rigid, BSA: globular, with protein tertiary structure) and surface charge density (SA > HA > BSA). The results of this study highlight the complexity of the interactions between NPs and minerals under different environments and provide valuable insights in understanding transport mechanisms and environmental fate of nanoplastics in aquatic environments.

1. Introduction

Plastics are extensively used in various fields, but are often ineluctably released into the environment due to mismanagement (Li et al., 2021a; Yu et al., 2019b). Most plastic debris can be broken down into smaller particles known as microplastics (1 μm – 5 mm) and further into nanoplastics (NPs; <1 μm) via physical, chemical, and biological processes (Singh et al., 2019). Nanoplastics have been regarded as emerging contaminants of global concern in aquatic and soil environments due to their high chemical stability, persistence, adsorption capacity, and bioavailability. Owing to the large specific surface area, high surface reactivity, abundant surface functional groups and adsorption sites, the ubiquitous existence of NPs pose great ecological risks to organisms and humans (Abdolahpur Monikh et al., 2020; Yu et al., 2019b). Thus, understanding NPs' environmental behavior is crucial for assessing their ecological risks.

Once entering into the environment, NPs inevitably undergo a series of aging, transport and deposition processes, which play an essential role in mediating their subsequent environmental fates and ecological risks (Gigault et al., 2021; Liu et al., 2019). Aging processes of NPs such as ultraviolet irradiation, biodegradation and chemical oxidation can alter their physicochemical properties, e.g., generating a large number of oxygen-containing functional groups, increasing surface negative charges, enhancing complexing ability and adsorption capacity for harmful contaminants (Li et al., 2022a; Luo et al., 2022; Zhang et al., 2022). The deposition behaviors of NPs in natural terrestrial and aquatic environments can be affected by their intrinsic properties (e.g., size, surface charges, functional groups), solution chemistry (e.g., pH, ionic strength and type), and coexisting organic macromolecules (OMs) and minerals (Li et al., 2022b; Sharma et al., 2021; Wu et al., 2022a; Wu et al., 2023b). As reported, pH and ionic strength had significant influences on the transport of NPs in aquatic systems. Cations and anions with various valence are ubiquitous in the natural aquatic media, which may play different roles on the transport and deposition behaviors of NPs (Li et al., 2022b; Wang et al., 2022b; Wu et al., 2023b; Zhao et al., 2021). However, to date, most studies focused on the impacts of cations on the deposition behaviors of NPs in aquatic systems, the roles and related mechanisms about anions are still limited. Minerals especially iron (hydr)oxides (e.g., goethite, ferrihydrite, hematite, and magnetite) with variable surface charge, and high specific surface area and surface reactivity, are universally present in terrestrial and aquatic environments, thus they could interact with NPs and affect the environmental behaviors of NPs (Li et al., 2021b; Nie et al., 2023). Furthermore, OMs (including humic substance, polysaccharide and protein), with numerous surface functional groups (such as hydroxyl, carboxyl, carbonyl, phenolic, and amino groups), are also pervasively distributed in natural environments with concentrations typically ranging from 0.1 to 10 mg/L. Organic macromolecules can strongly interact with iron (hydr)oxides to form Fe-OMs associations in natural aquatic and terrestrial environments via electrostatic interaction, ligand exchange-surface complexation, hydrogen bonding, and hydrophobic interaction, thereby resulting in changes in original surface properties and reactivity of iron (hydr)oxides (Bao et al., 2021; Philippe and Schaumann, 2014; Vindedahl et al., 2016). The interaction between iron (hydr)oxides minerals, OMs, and NPs may govern the transport, fate, and ecological risks of NPs, and thereby potentially alter the geochemical behaviors and toxicity of the associated contaminants in the environment (Abdolahpur Monikh et al., 2020; Bao et al., 2021; Ding et al., 2022; Liu et al., 2020; Wu et al., 2022b). In our previous work, we have systematically investigated the interactions between NPs and various iron (hydr)oxides minerals (hematite, goethite, magnetite, and ferrihydrite), and found that electrostatic interaction and ligand exchange were the dominant mechanism in the heteroaggregation of NPs with iron (hydr)oxides minerals. Humic acid could markedly suppressed heteroaggregation between NPs and iron (hydr)oxides minerals due to enhanced electrostatic repulsion, steric hindrance, and competition of surface attachment sites (Nie et al., 2023). Therefore, it is essential to gain a fundamental understanding of the roles of iron (hydr)oxides minerals, cations and anions as well as OMs in the transport and fate of NPs in the environment. Additionally, a molecular-level understanding of the deposition behaviors of aged NPs with iron (hydr)oxides minerals in the presence of various types of OMs under environmentally relevant conditions has a significant implication for the risk assessment of NPs.

Herein, carboxyl-modified polystyrene nanoplastics (COOH-PSNPs), the commonly used plastics and ubiquitous plastic contaminants in the environment, were selected as representative aged NPs in this study (Ding et al., 2022; Wu et al., 2020; Zhu et al., 2022). Goethite (α-FeOOH) is one of the most abundant iron containing mineral in soils and sediments (Cornell and Schwertmann, 2003; Uwayezu et al., 2019), thus was chosen as representative iron oxide mineral. Humic acid (HA), sodium alginate (SA), and bovine serum albumin (BSA), which are the major components of OMs in surface water, were selected as reasonable surrogates for humic substance, polysaccharide and protein, respectively (Liu et al., 2020). The effects of various solution chemistry conditions (pH and ionic type) and OMs on the deposition behavior of NPs with goethite were systematically investigated. The interaction mechanisms between COOH-PSNPs, goethite, and various OMs were elucidated and discussed.

2. Materials and methods

2.1. Materials

Goethite was synthesized according to the method described in supplementary material (Li et al., 2019). Carboxyl modified polystyrene nanoplastics (COOH-PSNPs, 2.5 % *w/v*) with an average diameter of 0.3 μm and humic acid were purchased from Shanghai Aladdin Biochemical Technology Co., Ltd. Sodium alginate and bovine serum albumin (fraction V, heat shock isolation) were purchased from Sangon Biotech (Shanghai) Co., Ltd. Other chemicals were purchased from Shanghai Chemical Reagent Corporation, China. All reagents were used as received. Ultrapure water was used in the study.

2.2. Characterization

Scanning electron microscopy (SEM, Scios, FEI Company) and

transmission electron microscope (TEM, G2 F20 S-TWIN, Tecnai) were used to examine the morphologies of samples. The zeta potentials of samples were measured by a high-sensitivity zeta potential analyzer (Omni, Brookhaven). The surface functional groups of samples were obtained using an attenuated total reflectance-Fourier transform infrared spectroscopy (ATR-FTIR, Vertex 70 spectrometer, BRUKER OPTICS). The ATR-FTIR scan time of background and sample always kept at 16 and 32 scans, respectively. Inductively coupled plasma-optical emission spectroscopy (ICP-OES, 700 Series, Agilent) was used to obtain the concentration of ions. The characterization results of COOH-PSNPs and goethite can be found in supplementary material.

2.3. Deposition experiments between COOH-PSNPs and goethite

The experiments were carried out in 250 mL conical flasks, where 0.01 g of goethite was added to a 100 mL solution of COOH-PSNPs. The concentration of COOH-PSNPs was set at 20 mg/L, a representative concentration of NPs commonly used in previous studies (Nie et al., 2023; Wang et al., 2022a). The study investigated the effects of pH, ionic type (including NaCl, KCl, $CaCl_2$, $NaNO_3$, Na_2SO_4, and Na_3PO_4), and organic macromolecules on the deposition between COOH-PSNPs and goethite through batch experiments. Since the pH of natural aquatic environments normally ranged from 5.0 to 9.0, a near-neutral reaction pH of 6.0 was selected in deposition experiments, except in the study of pH effect (Li et al., 2020). The concentration of ions is <10 mM in most real freshwater and could reach or above 10 mM in seawater (Hausmann et al., 2021; Wang et al., 2021). According to Wang et al. (2021), the effects of different ions (such as Na^+, Ca^{2+}, and SO_4^{2-}) on the stability of NPs can be distinguished in an ion concentration of 10 mM (Wang et al., 2021). In order to compare the impacts of ionic type at the same level, the concentration of various ions was 10 mM, a concentration which was usually employed in previous studies (Wang et al., 2021; Wang et al., 2022b; Zhao et al., 2021). The concentration of OMs ranged from 0 to 100 mg/L. To verify the roles of hydrogen bonding and hydrophobic interactions in the deposition process of COOH-PSNPs, various concentrations of urea (a hydrogen bonding breaker) and 50 % dimethyl sulfoxide (DMSO) (an dipolar aprotic organic solvent) were added into the solutions, respectively (Martin et al., 1967; Panuszko et al., 2019; Wu et al., 2023a; Zandieh and Liu, 2022). The initial pH of solution was adjusted by adding HCl or NaOH. The reaction solution was kept at 25 °C throughout the experiment. The mixtures were agitated in an orbital incubator shaker (ZWYR-D2403, Zhicheng) at 200 rpm. The suspension was sampled at different time intervals and centrifuged at 8000 rpm for 5 min to separate goethite from the solution of COOH-PSNPs. After that, 5 mL supernatants were taken out to measure the concentration of COOH-PSNPs using ultraviolet-visible spectrophotometry (UV-VIS, Cary 300, Agilent) at a wavelength of 230 nm (Nie et al., 2023). The difference between the initial concentrations (C_0) and suspended concentrations (C) of COOH-PSNPs at a given time was used to calculate the extent of deposition of COOH-PSNPs. The C/C_0 against the time (t) was used for plotting the normalized deposition curves. Each experiment was repeated twice. The solid specimens were dried at 30 °C, and their surface chemical groups and morphologies were further measured with ATR-FTIR, SEM, and TEM.

2.4. Quality control and quality assurance

For each batch of samples, one procedural blank, one matrix duplicate, and two spiked blanks were analyzed. Reported concentrations are average values obtained from two parallel experiments, and expressed as mean ± standard deviation. The recoveries of COOH-PSNPs were 98 ± 6 % in blank samples. No COOH-PSNPs were found in the procedural blank samples. All measure concentrations were not corrected with surrogate recoveries. All glassware used in the deposition experiments was soaked in 10 % aqua regia for >24 h and then thoroughly rinsed with deionized water to minimize cross-contamination prior to use (Nie et al., 2023).

3. Results and discussion

3.1. Effects of solution chemistry on deposition of COOH-PSNPs with goethite

3.1.1. Effect of pH

The deposition extent of COOH-PSNPs was highly pH-dependent (Fig. 1a). When pH was <6.0, the concentrations of COOH-PSNPs remaining in the suspensions significantly decreased with time when they were mixed with goethite, and 100 % of COOH-PSNPs deposited within 10 min. Both SEM (Fig. S1) and TEM (Fig. S2) images showed that COOH-PSNPs and goethite in suspension tend to form heteroaggregates, which could decrease the mobility and stability of COOH-PSNPs. However, the deposition extent gradually decreased with the increase of pH from 6.0 to 11.0, and only about 33 % of COOH-PSNPs deposited at pH 11.0 after 120 min, which were positively relevant with the zeta potentials of COOH-PSNPs and goethite (Fig. 2a). The zeta potential of COOH-PSNPs maintained at a highly negative value within the pH ranges (2.0–11.0), as a result of the dissociation of carboxyl groups on COOH-PSNPs surface (Zhu et al., 2022), and it decreased with an increase of pH, reaching −42.0 mV at pH 2.0 and −64.6 mV at pH 11.0, respectively. When pH increased from 3.0 to 5.0, the zeta potential of goethite was maintained at about 45.0 mV. As pH increased from 5.0 to 9.2 (the isoelectric point (pH_{IEP}) of goethite), the zeta potential values of goethite became less positive due to reduced protonation on goethite, indicating that the surface positive charges of goethite gradually became less, which resulted in a decrease of electrostatic attractions between COOH-PSNPs and goethite. When pH > pH_{IEP}, the surface charge of goethite became negative due to the deprotonation of Fe–OH, which could induce repulsive electrostatic forces between highly negatively charged COOH-PSNPs and goethite and thus prevent deposition (Uwayezu et al., 2019). This suggests that the electrostatic interactions played an important role in the deposition of COOH-PSNPs with goethite (Wu et al., 2022a; Wu et al., 2023b; Zhang et al., 2020).

3.1.2. Effect of ionic type

The universal occurrence of various cations and anions in estuarine and coastal waters is of great importance to affect the transport and fate of COOH-PSNPs in real aquatic environments. To thoroughly understand the influence of ionic type on the deposition of COOH-PSNPs with goethite, various representative cations (NaCl, KCl, or $CaCl_2$) and anions ($NaNO_3$, NaCl, Na_2SO_4, or Na_3PO_4) were added into the solution.

The deposition profiles of COOH-PSNPs with goethite were also established at pH 6.0 in the existence of various cations and anions. The deposition extent of COOH-PSNPs without any ions was significantly faster than that in the presence of 10 mM cations or anions. Without the presence of ions, COOH-PSNPs were deposited completely by goethite within 10 min. With the addition of NaCl, KCl, or $CaCl_2$, approximately 95 %, 94 %, and 89 % of COOH-PSNPs were deposited after 120 min, respectively (Fig. 1b). Divalent cations (Ca^{2+}) showed higher inhibitory effects on deposition extent of COOH-PSNPs than monovalent cations (Na^+, K^+). By adding $NaNO_3$, NaCl, Na_2SO_4, or Na_3PO_4, approximately 95 %, 95 %, 70 %, and 40 % of COOH-PSNPs deposited after 120 min, respectively (Fig. 1c).

In the presence of no cations, Na^+, K^+, or Ca^{2+} at pH 6.0, the zeta potential of goethite was 32.2, 20.3, 14.4, and 1.4 mV, while the zeta potential of COOH-PSNPs was −59.3, −60.6, −63.8, and −33.6 mV, respectively (Fig. 2b). The zeta potentials of goethite and COOH-PSNPs became less positive and negative as the ion valence rose, respectively. This can be attributed to more significant compression of electric double layer by divalent ions in comparison to monovalent ions. Cations with the same valence had parallel abilities to neutralize surface negative charges of COOH-PSNPs according to the Derjaguin–Landau–Verwey–Overbeek (DLVO) theory (Zhu et al., 2022),

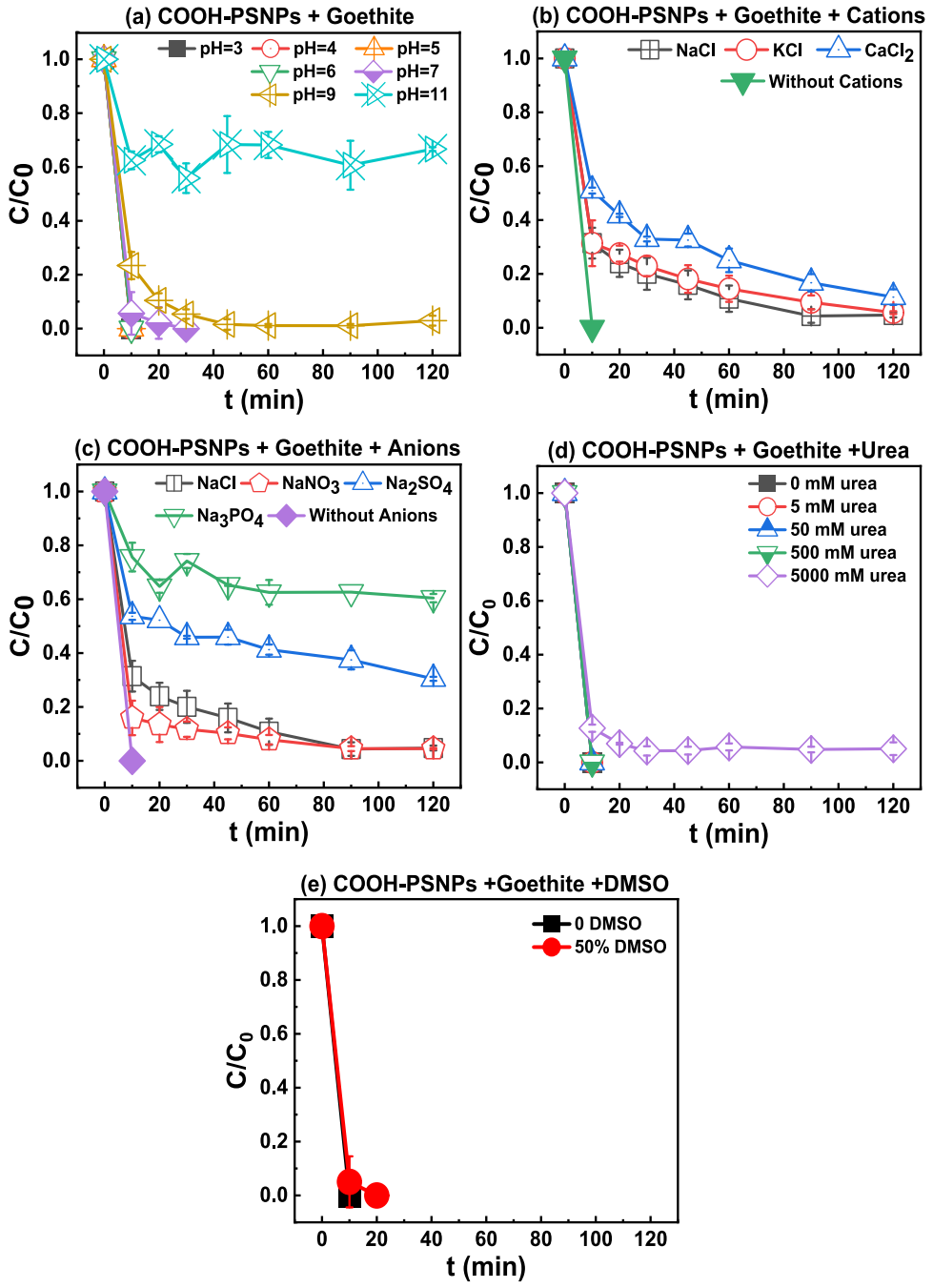

Fig. 1. Deposition curves of COOH-PSNPs with goethite: (a) at different pHs; in the presence of different (b) cations, (c) anions, (d) urea, and (e) DMSO concentrations at pH 6.0.

while divalent cations exhibited stronger capacities to neutralize surface negative charges than monovalent cations (Tan et al., 2021; Wu et al., 2020). Hence, the decreased deposition extent of COOH-PSNPs with goethite obtained with addition of multivalent cations suggests the dominant role of electrostatic forces.

Similarly, the effects of the anions on the COOH-PSNPs interaction were also found to be correlated with their zeta potentials. The zeta potential of COOH-PSNPs at pH 6.0 showed no significant changes in response to the addition of different anions. The zeta potential of goethite in the presence of no anions, $NaNO_3$, NaCl, Na_2SO_4, or Na_3PO_4 was 32.2, 14.9, 20.3, −28.1, and −38.2 mV, respectively (Fig. 2c). In the presence of $NaNO_3$ or NaCl, the deposition extent of COOH-PSNPs decreased as a result of the reduction of electrostatic attractions between goethite and COOH-PSNPs. The special interaction between SO_4^{2-} or $H_2PO_4^-$ (the existence form of phosphate at pH 6.0) with goethite can be found in Fig. S3. Briefly, after interaction with goethite for 120 min, the concentration of $H_2PO_4^-$ and SO_4^{2-} reduced by about 5 % and 3 %, respectively, indicating that both $H_2PO_4^-$ and SO_4^{2-} could be absorbed by goethite. Specific adsorption of SO_4^{2-} or $H_2PO_4^-$ on goethite could penetrate the electric double layer (EDL) more easily and neutralize surface positive charges more effectively, and even cause a potential reversal of goethite from positive to negative (Wang et al., 2018; Zhang and Peak, 2007; Zhu et al., 2022). This led to the electrostatic forces between COOH-PSNPs and goethite altered from attraction to repulsion in the presence of Na_2SO_4 and Na_3PO_4, thus significantly lowered the deposition of COOH-PSNPs.

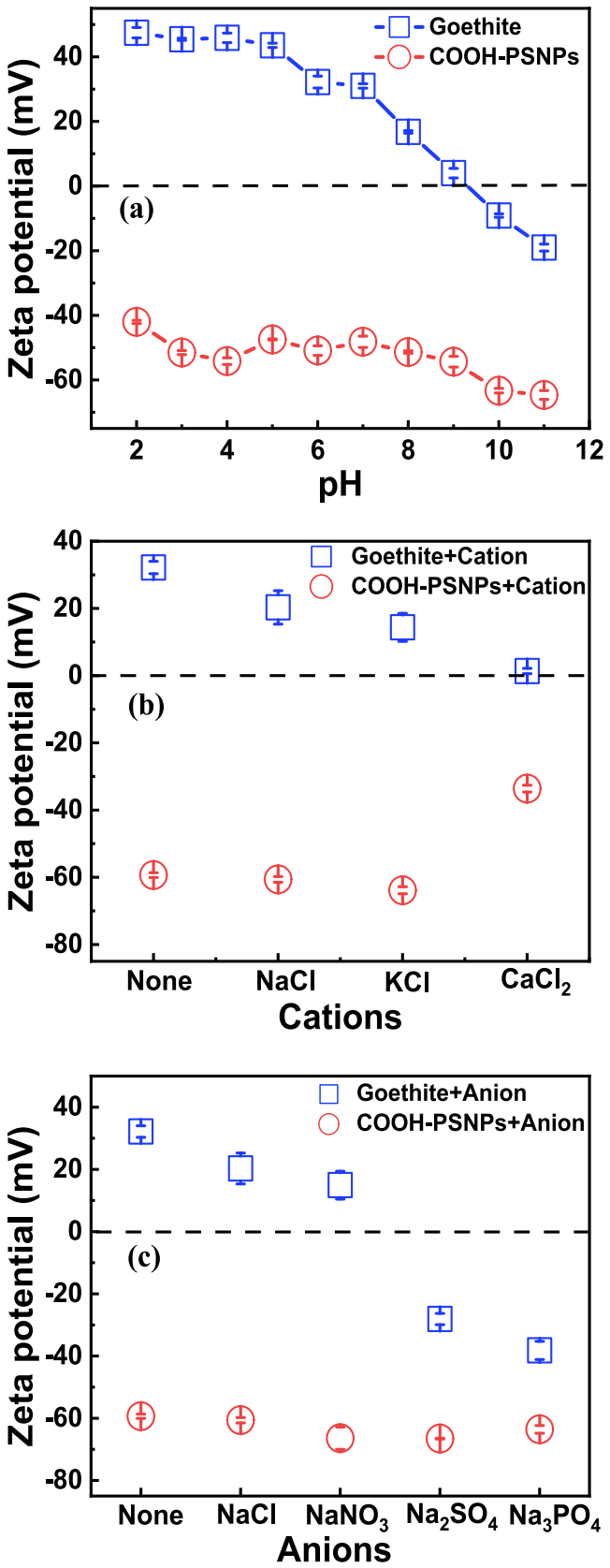

Fig. 2. Zeta potentials of COOH-PSNPs and goethite: (a) at different pH values; in the presence of various (b) cations, and (c) anions at pH 6.0.

3.1.3. Deposition mechanisms of COOH-PSNPs with goethite

The above results indicated that electrostatic interactions dominated for the deposition of COOH-PSNPs with goethite. However, although both goethite and COOH-PSNPs were negatively charged at pH 11.0 (Fig. 2a), and were thereby expected to electrostatically repel each other, approximately 33 % COOH-PSNPs could still be deposited. Therefore, electrostatic interaction alone cannot explain the decreased COOH-PSNPs concentration in the suspensions in relatively high pH. Various mechanisms, including electrostatic interactions, Van der Waals forces, hydrogen bonding, and chemical bonds might contribute to the deposition process of COOH-PSNPs. Abundant oxygen-containing functional groups (e.g., carboxyl and hydroxyl groups) on surface of COOH-PSNPs and goethite might form hydrogen bonds (i.e., –C–H···O—Fe, –C–O–H···O—Fe, and C—O···H–O–Fe) and induce Lewis acid-base interactions (Nie et al., 2023; Wu et al., 2022b; Zandieh and Liu, 2022). The ATR-FTIR spectra of goethite before and after mixing with COOH-PSNPs were further discussed in the section of Section 3.2.2. Formation of chemical bonds between –COOH on COOH-PSNPs and surface Fe coordinated –OH on goethite ($–FeOH_2^+ + RCOO^- \rightarrow –FeOOCR + H_2O$) may also be an important interaction mechanism for COOH-PSNPs with goethite (Bao et al., 2021; Lv et al., 2018; Wu et al., 2023b). Therefore, the electrostatic repulsions could be offset at high pH, which allows COOH-PSNPs to aggregate with goethite.

The deposition of COOH-PSNPs reached 100 % within 10 min at urea concentration of 0–500 mM, while almost 95 % COOH-PSNPs deposited after 120 min in the presence of 5000 mM urea, indicating that hydrogen bonding only plays a minor role in the deposition of COOH-PSNPs (Fig. 1d). COOH-PSNPs was deposited completely within 20 min with addition of 50 % DMSO, suggesting negligible function of hydrophobic interactions (Fig. 1e) (Martin et al., 1967; Panuszko et al., 2019; Wu et al., 2023a; Zandieh and Liu, 2022). Such results once again addressed the leading roles of electrostatic interactions and chemical bonds in the interaction of COOH-PSNPs and goethite (Wu et al., 2023b).

3.2. Effects of organic macromolecules on deposition of COOH-PSNPs with goethite

3.2.1. Deposition profiles of COOH-PSNPs with organic macromolecules

As shown in Fig. 3a, the deposition extent of COOH-PSNPs clearly decreased with increasing HA concentration from 0 to 0.5 mg/L. Approximately 100 %, 81 %, and 13 % COOH-PSNPs deposited in the presence of 0, 0.2, and 0.5 mg/L HA, respectively. By increasing of SA concentration from 0 to 0.1 mg/L, the stability of COOH-PSNPs enhanced steadily in mixture solution containing goethite. For instance, with addition of 0, 0.01, 0.02, and 0.05 mg/L SA, 100 % deposition of COOH-PSNPs with goethite could be reached after 10, 45, 90, and 120 min, respectively. Only 17 % of COOH-PSNPs deposited after 120 min when SA concentration was up to 0.1 mg/L (Fig. 3b). The deposition of COOH-PSNPs also remarkably retarded with increasing BSA concentration from 0 to 5 mg/L (Fig. 3c). For instance, 100 %, 96 %, and 16 % COOH-PSNPs were deposited after 120 min with addition of 0, 2, and 5 mg/L BSA, respectively. The concentration of COOH-PSNPs in the supernatant remained almost unchanged with time when HA, SA, or BSA concentration exceeded 0.5, 0.1, and 5 mg/L, respectively, suggesting that high OMs concentration could significantly inhibit the deposition of COOH-PSNPs with goethite. Fig. 4 shows the SEM images of goethite before and after mixed with COOH-PSNPs in the presence of different OMs concentrations. The number of COOH-PSNPs-goethite heteroaggregates reduced remarkably with increasing OMs concentration, and any COOH-PSNPs-goethite heteroaggregates cannot be observed since the HA, SA, and BSA concentration exceeded 0.5, 0.1, and 5 mg/L, respectively, which further confirms the decreased deposition of COOH-PSNPs with goethite.

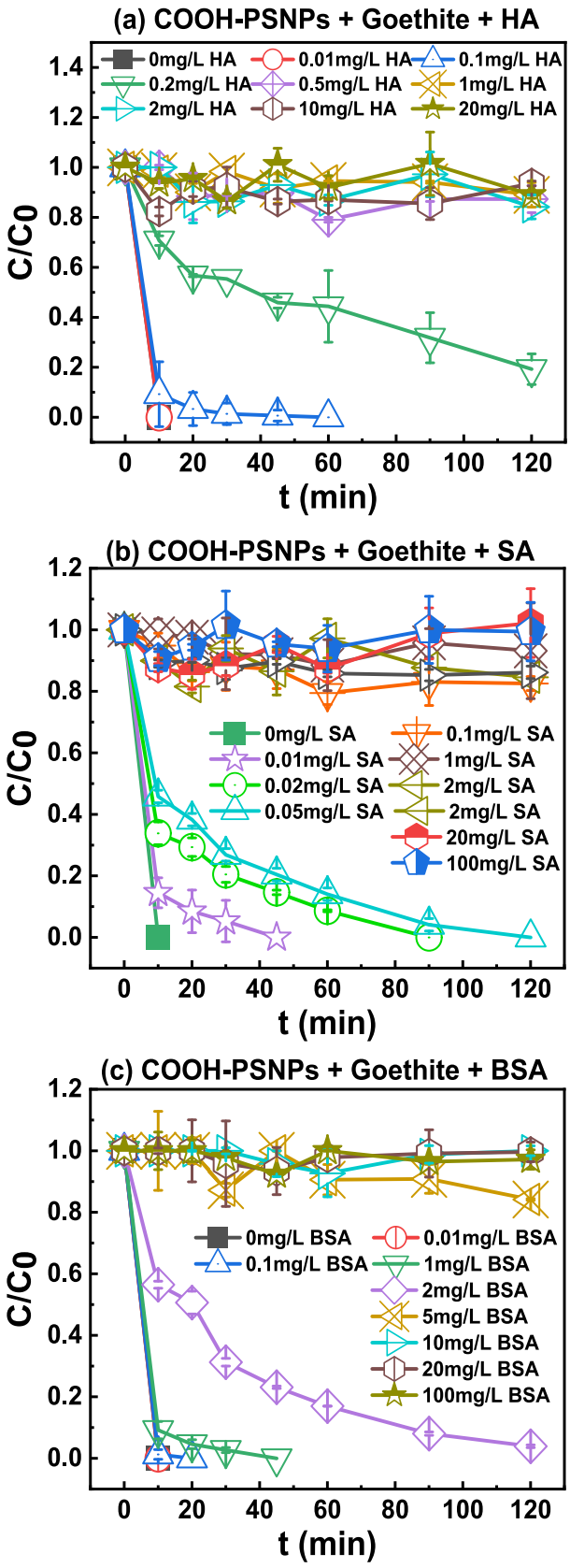

Fig. 3. Deposition curves of COOH-PSNPs with goethite in the presence of different concentrations of (a) HA, (b) SA, and (c) BSA at pH 6.0.

3.2.2. *Deposition mechanisms of COOH-PSNPs with organic macromolecules*

Organic macromolecules tend to interact with mineral surface, which can modify the surface physicochemical properties and reactivity of minerals, thus affecting the deposition behavior of COOH-PSNPs with goethite (Lee and Hur, 2020). To obtain the detailed insights on the surface charge characteristics of COOH-PSNPs and goethite in the presence of OMs, their zeta potentials were systematically measured by adding different concentrations OMs. The zeta potential of HA (−44.6 mV), SA (−52.0 mV), and BSA (−20.5 mV) were negative at pH 6.0 (Fig. 5) due to the presence of a large number of negatively charged carboxylic acid (–COOH) and phenolic (–OH) functional groups on their surfaces. After mixed with OMs, zeta potential of goethite was gradually changed from positive to negative and was close to the value of pure OMs with increasing OMs concentration in the solution at pH 6.0. This indirectly implied that a positively charged goethite surface can adsorb OMs through electrostatic interaction and ligand exchange (Bao et al., 2021). Sorbed OMs could neutralize the positive charges on a goethite surface or even cause a reversal of surface charge from positive to negative at higher concentrations of OMs. Moreover, ligand exchange between hydroxyl groups on goethite surface with carboxylic acid (–COOH) and phenolic (–OH) functional groups on OMs surfaces, which may provide fewer hydroxyl groups on goethite surface for protonation, could also be partly responsible for the decreased zeta potential (Yang and Xing, 2009). Increasing the concentrations of OMs also resulted in the shifted pH_{IEP} of goethite to lower pH and more negative charges on the goethite surface apparently. For instance, in the presence of 0, 0.01, 0.1, 1,10, and 100 mg/L HA, the zeta potential of goethite at pH 6.0 was 32.2, 30.9, −9.8, −32.0, −42.4, and −49.4 mV, respectively (Fig. 5a). Similar trend of the zeta potentials of goethite can be seen with addition of SA (Fig. 5b) and BSA (Fig. 5c). There was no substantial difference in the zeta potentials of COOH-PSNPs in the presence versus absence of HA or SA (Fig. 5d and e), indicating that HA and SA exerted a negligible effect on the surface charge density of COOH-PSNPs. Increasing the BSA concentration slightly shifted the zeta potential of COOH-PSNPs to a less negative value, suggesting that the positively charged aromatic amino acids residues of BSA could complex with COOH-PSNPs (Fig. 5f) (Li et al., 2021a). Consequently, it can be assumed that the decreased deposition of COOH-PSNPs with increasing OMs concentration is related to the enhanced electrostatic repulsions between COOH-PSNPs and goethite (Loosli et al., 2013; Tan et al., 2021).

To better understand the deposition mechanisms of COOH-PSNPs with goethite, ATR-FTIR spectra of goethite before and after mixing with COOH-PSNPs were systematically investigated in the absence and presence of HA, SA, and BSA (Figs. S4 and 6). The typical adsorption peaks at 619, 792, 889, 1654, and 3138 cm^{-1} can be found on goethite. The peaks at 619 cm^{-1} were ascribed to the stretching vibration of Fe−O. The peaks at 792 and 889 cm^{-1} belonged to the outward and inward bending vibration of Fe−OH, respectively. The bending vibration of H − O − H was observed at the peaks of 1654 cm^{-1}. The board adsorption peak at 3138 cm^{-1} belonged to the stretching vibration of Fe−OH (Zhang et al., 2020; Zhang et al., 2022). For COOH-PSNPs, the peaks at 540, 698, 758, 1197, and 2920 cm^{-1} represented C−H vibrations, the peaks at 1452, 1492, and 1601 cm^{-1} were ascribed to the aromatic structure, and a peak at 1728 cm^{-1} corresponded to O−C=O stretching vibration of carboxyl groups (Zhu et al., 2022). More details about typical peaks of HA, SA, and BSA were provided in supplementary material Fig. S4.

For comparison, the interaction mechanisms between different OMs and goethite were studied by ATR-FTIR spectra (Fig. S4). After interaction with goethite, the adsorption peaks of C−O stretching vibration (1020 and 1024 cm^{-1}) and −OH vibration (3300 cm^{-1}) for HA and SA disappeared distinctly, while the position of C−O bending vibration for BSA shifted from 1390 to 1400–1421 cm^{-1}. Furthermore, the stretching band of –COOH for three kinds of OMs shifted to different degrees. For instance, the peaks at 1355, and 1552 cm^{-1} of HA shifted to 1425–1377,

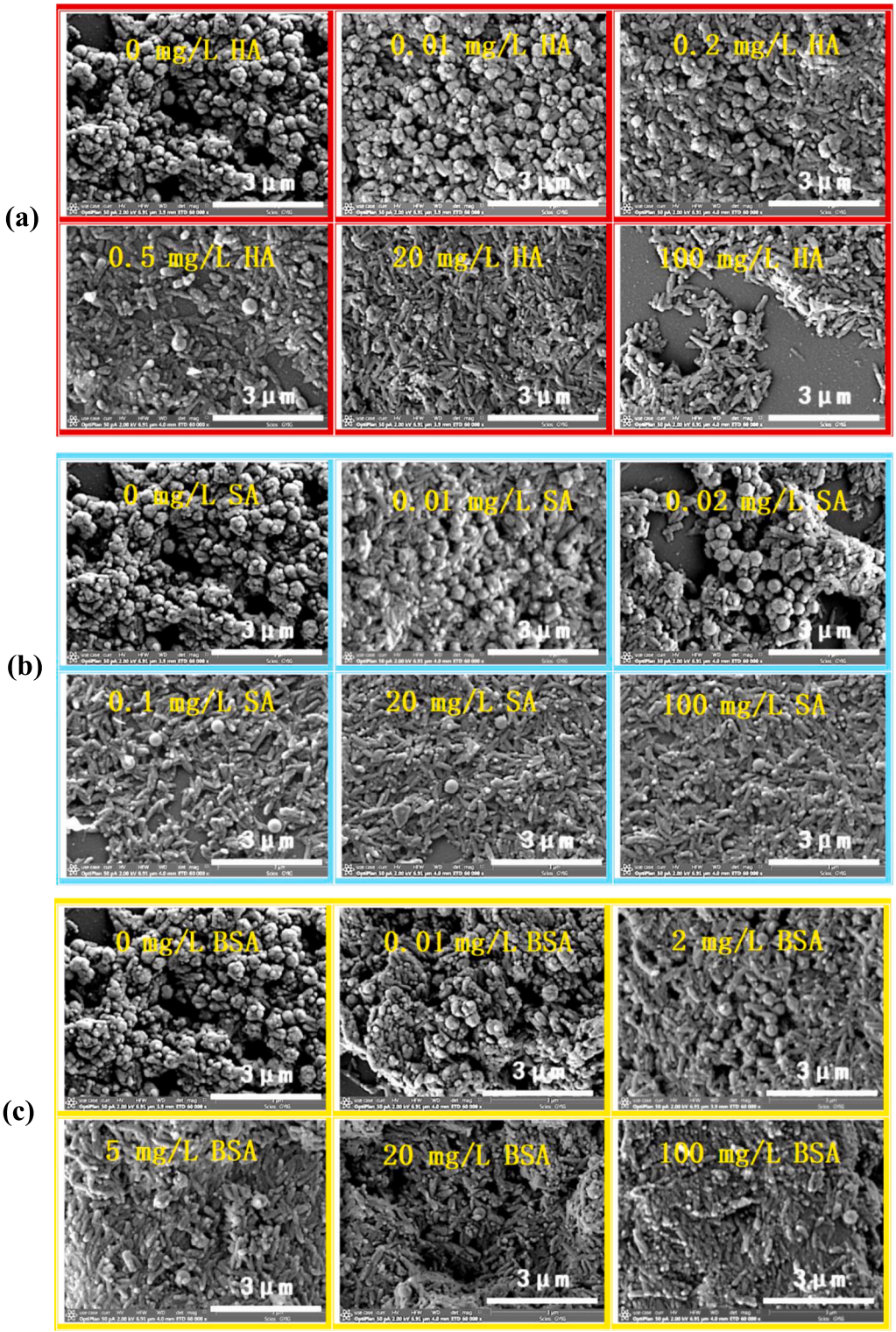

Fig. 4. Scanning electron microscopy images of goethite after interaction with COOH-PSNPs in the presence of different concentrations of (a) HA, (b) SA, and (c) BSA for 120 min at pH 6.0.

and 1610–1595 cm^{-1}, respectively. Moreover, not only the position of amide band I (1637 cm^{-1}) and II (1529 cm^{-1}) vibration of BSA changed in various degrees but also the intensity of amino groups on goethite gradually strengthened as BSA concentration increased, indicating that BSA was adsorbed on the surface of goethite. Such phenomena implied that new bonds were formed during the interaction between goethite and OMs. These results indicated that OMs can be adsorbed onto goethite by the interaction between ≡Fe–OH on goethite and oxygen-containing functional groups (–COOH and phenolic–OH) or amino groups in OMs, forming inner-sphere complexes via hydrogen bonding or ligand exchange/surface complexation. Thus, electrostatic interaction, hydrogen bonding, and ligand exchange might be the dominant mechanisms for the adsorption of OMs onto goethite (Bao et al., 2021; Kang and Xing, 2008; Tang et al., 2016).

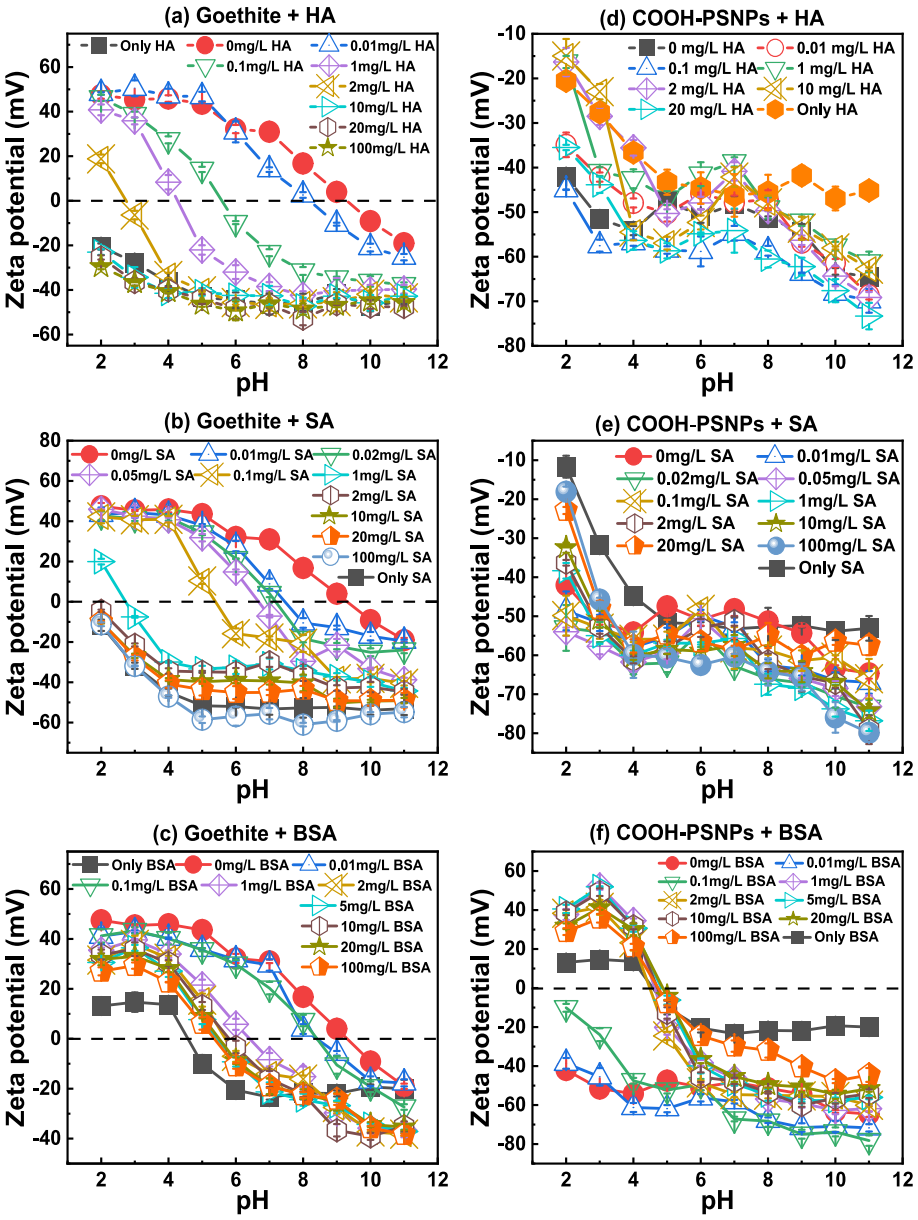

Fig. 5. Zeta potentials of goethite (a–c) and COOH-PSNPs (d–f) in the presence of different concentrations of organic macromolecules at different pH values.

All the position of goethite adsorption peaks did not shift significantly after interaction with COOH-PSNPs. Without OMs, the typical peaks of COOH-PSNPs appeared on goethite clearly without obvious alteration of position. With increasing OMs concentration, the peak intensity of the characteristic peaks related to COOH-PSNPs weakened gradually, whereas the typical peaks of OMs increased progressively (Fig. 6), indicating that fewer COOH-PSNPs and more OMs were adsorbed on goethite. For example, when HA concentration was up to 0.2 mg/L, almost no COOH-PSNPs adsorption peaks could be found on goethite, but the peak for HA at 1552 cm^{-1} improved gradually. Similar phenomena could be seen in SA and BSA when their concentrations were up to 0.1 and 2 mg/L, respectively. These results further confirmed that the deposition of COOH-PSNPs with goethite could be hindered by HA, SA, and BSA.

Both COOH-PSNPs and OMs can interact with goethite through ligand exchange or hydrogen bonding due to plentiful oxygen-containing functional groups (mainly –COOH and phenolic–OH) on their surfaces. OMs would be preferentially adsorbed onto goethite surface to compete for available binding sites (e.g., ≡Fe–OH) for COOH-PSNPs on goethite surface, consequently impairing the deposition of COOH-PSNPs with goethite (Bao et al., 2021; Prajapati et al., 2022).

Furthermore, the adsorption of OMs on the surface of COOH-PSNPs and goethite created strong steric hindrance between the adsorbed OMs on goethite and COOH-PSNPs, thus inhibiting the deposition of COOH-PSNPs (Liu et al., 2020; Singh et al., 2019; Wu et al., 2022a). A higher concentration of OMs led to more OMs adsorption on the surface of COOH-PSNPs and goethite and established a high repulsive energy barrier, hindering the interaction between COOH-PSNPs and goethite, resulting in a lower deposition extent. The presence of OMs can be visually corroborated by TEM images (Figs. S5–7). As the concentration of OMs elevated from 0 to 100 mg/L, the number of COOH-PSNPs-goethite aggregates decreased, corresponding to the lowered deposition extent, implying that the OMs provided more steric hindrance for inhibiting the deposition of COOH-PSNPs with goethite (Figs. S5a, S6a, and S7a). Furthermore, a gelatinous OMs layer intimately wrapped on the surface of the COOH-PSNPs-goethite aggregates could be clearly observed in the presence of OMs. Comparatively, increasing the concentration of OMs also resulted in a thicker adsorption layer of OMs on

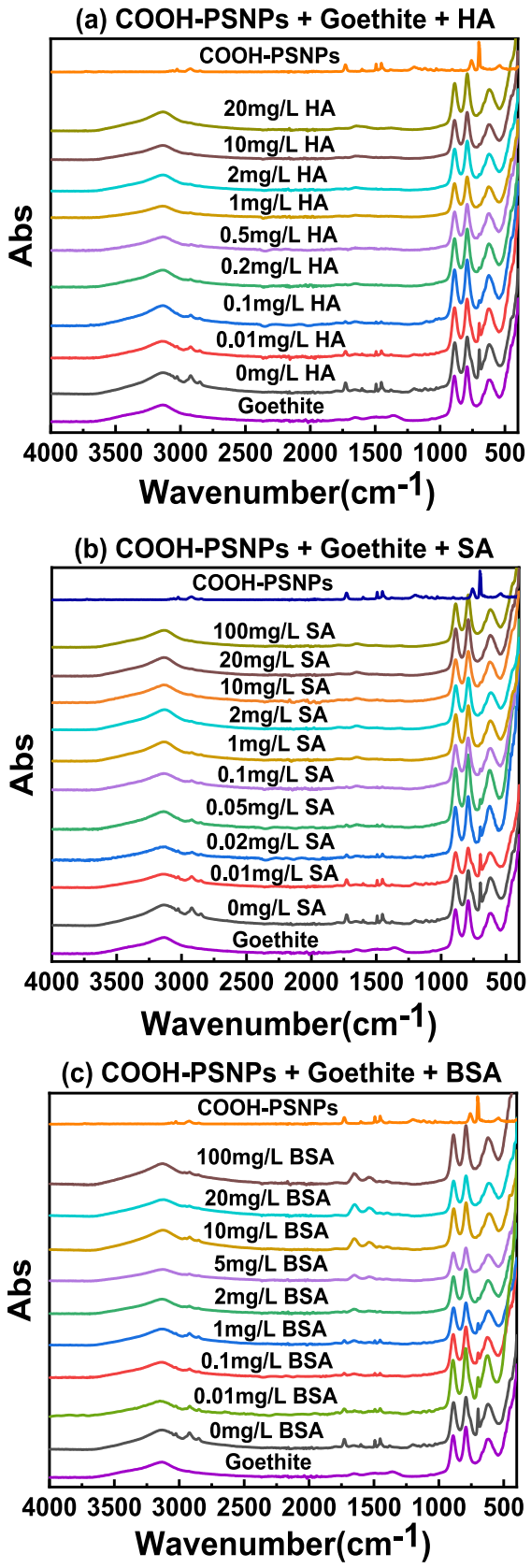

Fig. 6. Attenuated total reflectance - Fourier transform infrared spectroscopy of goethite after interaction with COOH-PSNPs in the presence of different concentrations of (a) HA, (b) SA, (c) BSA for 120 min at pH 6.0.

the surface of COOH-PSNPs (Figs. S5b, S6b, and S7b) and goethite (Figs. S5c, S6c, and S7c), demonstrating that OMs absorbed on both COOH-PSNPs and goethite. Although OMs and COOH-PSNPs were both negatively charged at pH 6.0, OMs may still adsorb on the surface of COOH-PSNPs through hydrophobic interaction, hydrogen bonding, and ligand exchange (Yu et al., 2019a). Besides, COOH-PSNPs gradually became adherent and surface deformed, and the edges of goethite became blurred. This layer of OMs can thus serve as a protective coating to prevent COOH-PSNPs deposition with goethite via steric repulsive force.

Overall, OMs coatings were found to hinder the deposition process between COOH-PSNPs and goethite due to enhanced electrostatic repulsion and steric hindrance. The suppression capacity of OMs is directly related to their concentrations. When the concentrations of OMs were insufficient to occupy the entire surface of goethite, COOH-PSNPs could still attach with goethite through electrostatic interactions. When the surface of goethite was completely occupied by OMs, the deposition of COOH-PSNPs with goethite was insignificant. Meanwhile, SA exhibited the highest inhibiting capacity on the deposition of COOH-PSNPs with goethite, followed by HA and BSA, and the minimum inhibitory concentrations for the deposition of COOH-PSNPs were 0.1, 0.5, and 5 mg/L for SA, HA, and BSA, respectively. This may be related to a higher electrostatic repulsion and steric hindrance originated from the SA layer than from HA and BSA, which was in accordance with the rank of their surface charge density: SA > HA > BSA (Duan et al., 2021). For instance, the zeta potential of goethite at pH 6.0 was −15.8, −9.8, and 29.9 mV in presence of 0.1 mg/L SA, HA, and BSA, respectively. The structural and physicochemical differences within HA (semi-rigid with globular structure macromolecule), SA (semi-flexible and linear macromolecule), BSA (globular macromolecule with protein tertiary structure) may also play crucial roles in their reaction (Liu et al., 2020; Wu et al., 2021). The flexible and linear macromolecule is prone to attach to COOH-PSNPs and goethite surface (Liu et al., 2020). Thus, a higher adsorption capacity and steric hindrance on COOH-PSNPs and goethite surface could be obtained for SA as compared with HA and BSA.

Therefore, based on the aforementioned discussion, it can be concluded that the decreased deposition extent of COOH-PSNPs with goethite in the presence of OMs is probably caused jointly by multiple mechanisms, including enhanced electrostatic repulsion and steric hindrance between COOH-PSNPs and OMs-coated goethite surface, and competition of surface binding sites on goethite between COOH-PSNPs and OMs (Dong et al., 2019; Singh et al., 2021; Yu et al., 2021). OMs play vital roles in mediating the environmental behavior of COOH-PSNPs in natural environments, and typical environmental concentrations of OMs would greatly enhance the mobility of COOH-PSNPs and modify their physicochemical properties, transportation, and bioavailability. Additionally, due to the complicated components in realistic scenarios of natural water and soil, such as the coexistence of various ions, OMs, inorganic colloids, and minerals may contribute to the stability of PSNPs, more parameters should be considered for elucidating the exact environmental behavior of PSNPs in natural ecosystems.

4. Conclusions

Our results indicate that the positively charged goethite can form heteroaggregates with COOH-PSNPs. Solution chemistry and organic macromolecules play substantial roles in the deposition process. With increasing pH, the deposition extent of COOH-PSNPs gradually reduced. The addition of cations and anions bid a hindrance in the deposition behaviors of COOH-PSNPs with goethite. The inhibition effects are positive with ions valence. Organic macromolecules also exhibited negative effects for the deposition of COOH-PSNPs, following the orders of SA > HA > BSA, which can be explained by electrostatic interactions, steric hindrance, ligand exchange, hydrogen bonding, and competitive adsorption sites. These findings reveal that the interaction between NPs and minerals in aquatic system is complicated, and further

investigations using other nanoplastics, natural organic matter, and minerals are necessary to elucidate the interaction between NPs and minerals. Furthermore, due to various ions and organic matter might alter the environmental behaviors of NPs, further experiments should be performed in the presence of various harmful organic pollutants, heavy metals, plastic additives, and pathogenic microorganisms for better understanding the environmental behaviors and ecological risk of NPs as well as associated pollutants under real environment.

CRediT authorship contribution statement

Ruiyin Xie: Methodology, Data curation, Writing-original draft. **Xiaohui Xing**: Methodology, Data curation, Writing-original draft. **Xin Nie**: Conceptualization, Data curation, Methodology, Visualization, Formal analysis, Investigation, Writing – original draft, Writing – review & editing, Project administration. **Xunsong Ma**: Data curation. **Quan Wan**: Manuscript revision, Project administration. **Qingsong Chen**: Manuscript revision. **Zixiong Li**: Manuscript revision. **Jingxin Wang**: Conceptualization, Methodology, Writing – original draft, Writing – review & editing.

Declaration of competing interest

The authors declare that they have no known competing financial interests or personal relationships that could have appeared to influence the work reported in this paper.

Data availability

Data will be made available on request.

Acknowledgments

The present study was financially supported by the B-type Strategic Priority Program of the Chinese Academy of Sciences (No. XDB41000000), National Natural Science Foundation of China (Nos. 41902041 and 41872046), Guizhou Provincial Science and Technology Projects (No. [2020]1Z039), Innovation Team of Ordinary Universities in Guangdong Province (No. 2020KCXTD022).

Appendix A. Supplementary data

Supplementary data to this article can be found online at https://doi.org/10.1016/j.scitotenv.2023.166783.

References

Abdolahpur Monikh, F., Vijver, M.G., Guo, Z., Zhang, P., Darbha, G.K., Peijnenburg, W., 2020. Metal sorption onto nanoscale plastic debris and trojan horse effects in Daphnia magna: role of dissolved organic matter. Water Res. 186, 116410 https://doi.org/10.1016/j.watres.2020.116410.

Bao, Y.P., Bolan, N.S., Lai, J.H., Wang, Y.S., Jin, X.H., Kirkham, M.B., Wu, X.L., Fang, Z., Zhang, Y., Wang, H.L., 2021. Interactions between organic matter and Fe (hydr) oxides and their influences on immobilization and remobilization of metal(loid)s: a review. Crit. Rev. Environ. Sci. Technol. 52 (22), 4016–4037. https://doi.org/10.1080/10643389.2021.1974766.

Cornell, R.M., Schwertmann, U., 2003. The Iron Oxides: Structure, Properties, Reactions, Occurences and Uses. Wiley-VCH GmbH& Co. KGaA, Weinheim. https://doi.org/10.1002/3527602097.

Ding, L., Luo, Y., Yu, X., Ouyang, Z., Liu, P., Guo, X., 2022. Insight into interactions of polystyrene microplastics with different types and compositions of dissolved organic matter. Sci. Total Environ. 824, 153883 https://doi.org/10.1016/j.scitotenv.2022.153883.

Dong, Z., Zhang, W., Qiu, Y., Yang, Z., Wang, J., Zhang, Y., 2019. Cotransport of nanoplastics (NPs) with fullerene (C60) in saturated sand: effect of NPs/C60 ratio and seawater salinity. Water Res. 148, 469–478. https://doi.org/10.1016/j.watres.2018.10.071.

Duan, Z., Wang, P., Yu, G., Liang, M., Dong, J., Su, J., Huang, W., Li, Y., Zhang, A., Chen, C., 2021. Aggregation kinetics of UV-aged soot nanoparticles in wet environments: effects of irradiation time and background solution chemistry. Water Res. 201, 117385 https://doi.org/10.1016/j.watres.2021.117385.

Gigault, J., El Hadri, H., Nguyen, B., Grassl, B., Rowenczyk, L., Tufenkji, N., Feng, S., Wiesner, M., 2021. Nanoplastics are neither microplastics nor engineered nanoparticles. Nat. Nanotechnol. 16 (5), 501–507. https://doi.org/10.1038/s41565-021-00886-4.

Hausmann, J.N., Schlögl, R., Menezes, P.W., Driess, M., 2021. Is direct seawater splitting economically meaningful? Energy Environ. Sci. 14 (7), 3679–3685. https://doi.org/10.1039/d0ee03659e.

Kang, S.H., Xing, B.S., 2008. Humic acid fractionation upon sequential adsorption onto goethite. Langmuir 24 (6), 2525–2531. https://doi.org/10.1021/la702914q.

Lee, Y.K., Hur, J., 2020. Adsorption of microplastic-derived organic matter onto minerals. Water Res. 187, 116426 https://doi.org/10.1016/j.watres.2020.116426.

Li, M., He, L., Zhang, M., Liu, X., Tong, M., Kim, H., 2019. Cotransport and deposition of Iron oxides with different-sized plastic particles in saturated quartz sand. Environ. Sci. Technol. 53 (7), 3547–3557. https://doi.org/10.1021/acs.est.8b06904.

Li, X., He, E., Xia, B., Van Gestel, C.A.M., Peijnenburg, W.J.G.M., Cao, X., Qiu, H., 2020. Impact of CeO2 nanoparticles on the aggregation kinetics and stability of polystyrene nanoplastics: importance of surface functionalization and solution chemistry. Water Res. 186, 116324 https://doi.org/10.1016/j.watres.2020.116324.

Li, X., He, E., Jiang, K., Peijnenburg, W., Qiu, H., 2021a. The crucial role of a protein corona in determining the aggregation kinetics and colloidal stability of polystyrene nanoplastics. Water Res. 190, 116742 https://doi.org/10.1016/j.watres.2020.116742.

Li, M., Zhang, X., Yi, K., He, L., Han, P., Tong, M., 2021b. Transport and deposition of microplastic particles in saturated porous media: co-effects of clay particles and natural organic matter. Environ. Pollut. 287, 117585 https://doi.org/10.1016/j.envpol.2021.117585.

Li, X., Ji, S., He, E., Peijnenburg, W., Cao, X., Zhao, L., Xu, X., Zhang, P., Qiu, H., 2022a. UV/ozone induced physicochemical transformations of polystyrene nanoparticles and their aggregation tendency and kinetics with natural organic matter in aqueous systems. J. Hazard. Mater. 433, 128790 https://doi.org/10.1016/j.jhazmat.2022.128790.

Li, S., Yang, M., Wang, H., Jiang, Y., 2022b. Adsorption of microplastics on aquifer media: effects of the action time, initial concentration, ionic strength, ionic types and dissolved organic matter. Environ. Pollut. 308, 119482 https://doi.org/10.1016/j.envpol.2022.119482.

Liu, Y., Hu, Y., Yang, C., Chen, C., Huang, W., Dang, Z., 2019. Aggregation kinetics of UV irradiated nanoplastics in aquatic environments. Water Res. 163, 114870 https://doi.org/10.1016/j.watres.2019.114870.

Liu, Y., Huang, Z., Zhou, J., Tang, J., Yang, C., Chen, C., Huang, W., Dang, Z., 2020. Influence of environmental and biological macromolecules on aggregation kinetics of nanoplastics in aquatic systems. Water Res. 186, 116316 https://doi.org/10.1016/j.watres.2020.116316.

Loosli, F., Le Coustumer, P., Stoll, S., 2013. TiO2 nanoparticles aggregation and disaggregation in presence of alginate and Suwannee River humic acids. pH and concentration effects on nanoparticle stability. Water Res. 47 (16), 6052–6063. https://doi.org/10.1016/j.watres.2013.07.021.

Luo, H., Liu, C., He, D., Xu, J., Sun, J., Li, J., Pan, X., 2022. Environmental behaviors of microplastics in aquatic systems: a systematic review on degradation, adsorption, toxicity and biofilm under aging conditions. J. Hazard. Mater. 423 (Pt A), 126915 https://doi.org/10.1016/j.jhazmat.2021.126915.

Lv, J., Miao, Y., Huang, Z., Han, R., Zhang, S., 2018. Facet-mediated adsorption and molecular fractionation of humic substances on hematite surfaces. Environ. Sci. Technol. 52 (22), 13662. https://doi.org/10.1021/acs.est.8b03940.

Martin, D., Weise, A., Niclas, H.J., 1967. The solvent dimethyl sulfoxide. Angew. Chem. Int. Ed. Engl. 6 (4), 318–334. https://doi.org/10.1002/anie.196703181.

Nie, X., Xing, X., Xie, R., Wang, J., Yang, S., Wan, Q., Zeng, E.Y., 2023. Impact of iron/aluminum (hydr)oxide and clay minerals on heteroaggregation and transport of nanoplastics in aquatic environment. J. Hazard. Mater. 130649 https://doi.org/10.1016/j.jhazmat.2022.130649.

Panuszko, A., Bruździak, P., Śmiechowski, M., Stasiulewicz, M., Stefaniak, J., Stangret, J., 2019. DMSO hydration redefined: unraveling the hydrophobic hydration of solutes with a mixed hydrophilic–hydrophobic characteristic. J. Mol. Liq. 294 https://doi.org/10.1016/j.molliq.2019.111661.

Philippe, A., Schaumann, G.E., 2014. Interactions of dissolved organic matter with natural and engineered inorganic colloids: a review. Environ. Sci. Technol. 48 (16), 8946–8962. https://doi.org/10.1021/es502342r.

Prajapati, A., Narayan Vaidya, A., Kumar, A.R., 2022. Microplastic properties and their interaction with hydrophobic organic contaminants: a review. Environ. Sci. Pollut. Res. 29 (33), 49490–49512. https://doi.org/10.1007/s11356-022-20723-y.

Sharma, V.K., Ma, X., Guo, B., Zhang, K., 2021. Environmental factors-mediated behavior of microplastics and nanoplastics in water: a review. Chemosphere 271, 129597. https://doi.org/10.1016/j.chemosphere.2021.129597.

Singh, N., Tiwari, E., Khandelwal, N., Darbha, G.K., 2019. Understanding the stability of nanoplastics in aqueous environments: effect of ionic strength, temperature, dissolved organic matter, clay, and heavy metals. Environ. Sci.-Nano 6 (10), 2968–2976. https://doi.org/10.1039/c9en00557a.

Singh, N., Khandelwal, N., Ganie, Z.A., Tiwari, E., Darbha, G.K., 2021. Eco-friendly magnetic biochar: an effective trap for nanoplastics of varying surface functionality and size in the aqueous environment. Chem. Eng. J. 418, 129405 https://doi.org/10.1016/j.cej.2021.129405.

Tan, M., Liu, L., Zhang, M., Liu, Y., Li, C., 2021. Effects of solution chemistry and humic acid on the transport of polystyrene microplastics in manganese oxides coated sand. J. Hazard. Mater. 413, 125410 https://doi.org/10.1016/j.jhazmat.2021.125410.

Tang, Z., Zhao, X., Zhao, T., Wang, H., Wang, P., Wu, F., Giesy, J.P., 2016. Magnetic nanoparticles interaction with humic acid: in the presence of surfactants. Environ. Sci. Technol. 50 (16), 8640–8648. https://doi.org/10.1021/acs.est.6b01749.

Uwayezu, J.N., Yeung, L.W.Y., Backstrom, M., 2019. Sorption of PFOS isomers on goethite as a function of pH, dissolved organic matter (humic and fulvic acid) and sulfate. Chemosphere 233, 896–904. https://doi.org/10.1016/j.chemosphere.2019.05.252.

Vindedahl, A.M., Stemig, M.S., Arnold, W.A., Penn, R.L., 2016. Character of humic substances as a predictor for goethite nanoparticle reactivity and aggregation. Environ. Sci. Technol. 50 (3), 1200–1208. https://doi.org/10.1021/acs.est.5b04136.

Wang, L., Putnis, C., Hövelmann, J., Putnis, A., 2018. Interfacial precipitation of phosphate on hematite and goethite. Minerals 8 (5), 207. https://doi.org/10.3390/min8050207.

Wang, J., Zhao, X., Wu, A., Tang, Z., Niu, L., Wu, F., Wang, F., Zhao, T., Fu, Z., 2021. Aggregation and stability of sulfate-modified polystyrene nanoplastics in synthetic and natural waters. Environ. Pollut. 268 https://doi.org/10.1016/j.envpol.2020.114240.

Wang, Y., Chen, X., Wang, F., Cheng, N., 2022a. Influence of typical clay minerals on aggregation and settling of pristine and aged polyethylene microplastics. Environ. Pollut. 316 (Pt 2), 120649 https://doi.org/10.1016/j.envpol.2022.120649.

Wang, X., Diao, Y., Dan, Y., Liu, F., Wang, H., Sang, W., Zhang, Y., 2022b. Effects of solution chemistry and humic acid on transport and deposition of aged microplastics in unsaturated porous media. Chemosphere 309 (Pt 2), 136658. https://doi.org/10.1016/j.chemosphere.2022.136658.

Wu, X., Lyu, X., Li, Z., Gao, B., Zeng, X., Wu, J., Sun, Y., 2020. Transport of polystyrene nanoplastics in natural soils: effect of soil properties, ionic strength and cation type. Sci. Total Environ. 707, 136065 https://doi.org/10.1016/j.scitotenv.2019.136065.

Wu, J., Jiang, R., Liu, Q., Ouyang, G., 2021. Impact of different modes of adsorption of natural organic matter on the environmental fate of nanoplastics. Chemosphere 263, 127967. https://doi.org/10.1016/j.chemosphere.2020.127967.

Wu, J., Liu, J., Wu, P., Sun, L., Chen, M., Shang, Z., Ye, Q., Zhu, N., 2022a. The heteroaggregation and deposition behavior of nanoplastics on Al(2)O(3) in aquatic environments. J. Hazard. Mater. 435, 128964 https://doi.org/10.1016/j.jhazmat.2022.128964.

Wu, J., Ye, Q., Wu, P., Xu, S., Liu, Y., Ahmed, Z., Rehman, S., Zhu, N., 2022b. Heteroaggregation of nanoplastics with oppositely charged minerals in aquatic environment: experimental and theoretical calculation study. Chem. Eng. J. 428, 131191 https://doi.org/10.1016/j.cej.2021.131191.

Wu, Y., Shi, Y., Wang, H., 2023a. Urea as a hydrogen bond producer for fabricating mechanically very strong hydrogels. Macromolecules 56 (12), 4491–4502. https://doi.org/10.1021/acs.macromol.3c00611.

Wu, J., Ye, Q., Li, P., Sun, L., Huang, M., Liu, J., Ahmed, Z., Wu, P., 2023b. The heteroaggregation behavior of nanoplastics on goethite: effects of surface functionalization and solution chemistry. Sci. Total Environ. 870, 161787 https://doi.org/10.1016/j.scitotenv.2023.161787.

Yang, K., Xing, B., 2009. Interactions of humic acid with nanosized inorganic oxides. Environ. Pollut. 157 (4), 1095–1100. https://doi.org/10.1016/j.envpol.2008.11.007.

Yu, S., Shen, M., Li, S., Fu, Y., Zhang, D., Liu, H., Liu, J., 2019a. Aggregation kinetics of different surface-modified polystyrene nanoparticles in monovalent and divalent electrolytes. Environ. Pollut. 255 (Pt 2), 113302 https://doi.org/10.1016/j.envpol.2019.113302.

Yu, F., Yang, C., Zhu, Z., Bai, X., Ma, J., 2019b. Adsorption behavior of organic pollutants and metals on micro/nanoplastics in the aquatic environment. Sci. Total Environ. 694, 133643 https://doi.org/10.1016/j.scitotenv.2019.133643.

Yu, S.J., Li, Q.C., Shan, W.Y., Hao, Z.N., Li, P., Liu, J.F., 2021. Heteroaggregation of different surface-modified polystyrene nanoparticles with model natural colloids. Sci. Total Environ. 784, 147190 https://doi.org/10.1016/j.scitotenv.2021.147190.

Zandieh, M., Liu, J., 2022. Removal and degradation of microplastics using the magnetic and Nanozyme activities of bare Iron oxide nanoaggregates. Angew. Chem. Int. Ed. 61 (47), e202212013 https://doi.org/10.1002/anie.202212013.

Zhang, G.Y., Peak, D., 2007. Studies of Cd(II)–sulfate interactions at the goethite–water interface by ATR-FTIR spectroscopy. Geochim. Cosmochim. Acta 71 (9), 2158–2169. https://doi.org/10.1016/j.gca.2006.12.020.

Zhang, Y., Luo, Y., Guo, X., Xia, T., Wang, T., Jia, H., Zhu, L., 2020. Charge mediated interaction of polystyrene nanoplastic (PSNP) with minerals in aqueous phase. Water Res. 178, 115861 https://doi.org/10.1016/j.watres.2020.115861.

Zhang, Y., Luo, Y., Yu, X., Huang, D., Guo, X., Zhu, L., 2022. Aging significantly increases the interaction between polystyrene nanoplastic and minerals. Water Res. 219, 118544 https://doi.org/10.1016/j.watres.2022.118544.

Zhao, P., Cui, L., Zhao, W., Tian, Y., Li, M., Wang, Y., Chen, Z., 2021. Cotransport and deposition of colloidal polystyrene microplastic particles and tetracycline in porous media: the impact of ionic strength and cationic types. Sci. Total Environ. 753, 142064 https://doi.org/10.1016/j.scitotenv.2020.142064.

Zhu, S., Mo, Y., Luo, W., Xiao, Z., Jin, C., Qiu, R., 2022. Aqueous aggregation and deposition kinetics of fresh and carboxyl-modified nanoplastics in the presence of divalent heavy metals. Water Res. 222, 118877 https://doi.org/10.1016/j.watres.2022.118877.